Atmospheric Environment 147 (2016) 458–469

Contents lists available at ScienceDirect

Atmospheric Environment

journal homepage: www.elsevier.com/locate/atmosenv

$PM_{2.5}$ from the Guanzhong Plain: Chemical composition and implications for emission reductions

Xinyi Niu [a, b], Junji Cao [b, c, d, *], Zhenxing Shen [e], Steven Sai Hang Ho [b, f], Xuexi Tie [b, c, g], Shuyu Zhao [b, c], Hongmei Xu [e, b], Ting Zhang [b, c], Rujin Huang [b, c]

[a] School of Human Settlements and Civil Engineering, Xi'an Jiaotong University, Xi'an, 710049, China
[b] Key Lab of Aerosol Chemistry & Physics, Institute of Earth Environment, Chinese Academy of Sciences, Xi'an, 710061, China
[c] State Key Lab of Loess and Quaternary Geology (SKLLQG), Institute of Earth Environment, Chinese Academy of Sciences, Xi'an, 710061, China
[d] Institute of Global Environmental Change, Xi'an Jiaotong University, Xi'an, 710049, China
[e] Department of Environmental Science and Engineering, Xi'an Jiaotong University, Xi'an, 710049, China
[f] Division of Atmospheric Sciences, Desert Research Institute, Reno, NV, 89512, United States
[g] National Center for Atmospheric Research, Boulder, CO, USA

HIGHLIGHTS

- One-year fine particulate matters ($PM_{2.5}$) sampling was conducted in Guanzhong Plain.
- Secondary aerosols from coal combustion and biomass burning were the major sources.
- Primary emissions and secondary aerosol precursors should be prior controlled.

ARTICLE INFO

Article history:
Received 2 May 2016
Received in revised form
1 September 2016
Accepted 15 October 2016
Available online 15 October 2016

Keywords:
Air pollution
Guanzhong plain
Episode
Secondary aerosol
Emission reduction

ABSTRACT

Atmospheric particulate matter (PM) affects important environmental issues including air quality, regional and global climates, and human health. A one-year sampling campaign for $PM_{2.5}$ was conducted at six locations in Guanzhong Plain, including the cities of Xi'an, Weinan and Baoji, from March 2012 to March 2013. The 24-h average $PM_{2.5}$ mass concentration was 134.7 μg m^{-3}, that substantially exceeds the National Ambient Air Quality Standard level of 35 μg m^{-3}. The highest loadings of both organic and elemental carbon (OC and EC) occurred in winter: EC co-varied with OC but showed less variability, presumably due to more stable emissions. The greatest contributions of secondary inorganic ions (SO_4^{2-}, NO_3^- and NH_4^+) to the total quantified ions also were seen in winter, presumably due to gaseous precursors from coal combustion and biomass burning. Two high PM episodes occurred, one in the autumn and the other in winter. During the autumn episode, regional pollution from biomass burning raised the concentrations of secondary ions while coal combustion was a strong influence during the winter episode. Modeling simulations suggest that the control measures on both primary emissions and secondary aerosol precursors including SO_2, NO_x, and NH_3 are needed to reduce the PM levels of the region.

1. Introduction

Atmospheric particulate matter (PM) is the major air pollutant in many Chinese cities due to the combined effects of rapid industrialization, the high population densities, and physical factors that lead to weak dilution and dispersion. Heavily-impacted regions include both developing and developed regions such as the North China Plain (NCP), the Yangtze River Delta region (YRD), the Pearl River Delta region (PRD) and the Guanzhong Plain (Li et al., 2011; Tie and Cao, 2010; van Donkelaar et al., 2010; Zhang et al., 2002; Zhao et al., 2013). Fine particulate matter ($PM_{2.5}$, PM with aerodynamic equivalent diameters of Dp < 2.5 μm) in these areas are mainly produced by anthropogenic activities. Epidemiological studies have shown that sustained exposure to high PM loadings, particularly fine and ultrafine particles ($PM_{0.1}$) can penetrate deeply into human lungs and lead to significant acute

* Corresponding author. Key Lab of Aerosol Chemistry & Physics, Institute of Earth Environment, Chinese Academy of Sciences, Xi'an, 710061, China.
E-mail address: cao@loess.llqg.ac.cn (J. Cao).

http://dx.doi.org/10.1016/j.atmosenv.2016.10.029
1352-2310/

and chronic health impacts on the respiratory and cardiovascular systems (Cao et al., 2012b; Harrison and Yin, 2000; Kelly and Fussell, 2012; Strak et al., 2012). High PM levels can be caused by direct emissions or by the formation of secondary aerosols; the latter are produced from gaseous precursors, especially sulfur dioxide (SO_2), nitrogen oxides (NO_x), ammonia (NH_3), and volatile organic compounds (VOCs), and they are mainly composed of sulfate, nitrate, ammonium, and organic carbon (Bi et al., 2007; Chan and Yao, 2008; Wang et al., 2012).

$PM_{2.5}$, emitted from vast number of sources, and the loadings of these aerosol particles not only reflect regional atmospheric characteristics but also affect the hemispheric to global environment through long-distance transport (Zhang et al., 2012; Zhao et al., 2013). Therefore, information on the chemical composition of $PM_{2.5}$ is valuable for determining the particles' sources, how they form, their physical/chemical characteristics and how they behave in the environment. In China, many aerosol studies have been conducted since 2000, and these include investigations of the $PM_{2.5}$ carbonaceous components (Cao et al., 2004; Zhang et al., 2008; Zhu et al., 2010, 2014), water-soluble inorganic ions (Han et al., 2016; Lai et al., 2007; Shen et al., 2009, 2011), trace elements (Duan et al., 2014; Zhai et al., 2014; Zhang et al., 2012), physical properties (Cao et al., 2015; Xiao et al., 2014) and sources (Ho et al., 2006; Song et al., 2007; Wang et al., 2014). In general, aerosol sulfate mainly forms through the oxidation of SO_2, which is emitted in large quantities from coal combustion, while nitrate is produced from NO_x, which is mainly produced by internal combustion engines and power plants. A study conducted in Xi'an, China showed that energy production was responsible for 46% of the secondary aerosol nitrate, and this source also contributed to the formation of secondary aerosol sulfate (Wang et al., 2014).

The Guanzhong Plain is situated in the central region of Shaanxi Province (an area of 34,000 km^2, with a population of 30 million), and it contains six major cities: Xi'an, Tongchuan, Baoji, Weinan, Xianyang, and Yangling. The temperate monsoonal climate of the region is dominated by the East Asian monsoon, and the annual rainfall is 500–800 mm. During winter and spring, northwesterly monsoonal winds often bring soil dust to the plain from the arid and semi-arid regions in Northwest China; and in summer and autumn, monsoonal winds from the southeast bring moisture to the region (Cao et al., 2008a; Shen et al., 2007). With the rapid increase in the number of motor vehicles in use and the growth in energy consumption during the past few decades, many parts of the plain have suffered serious air quality issues (Choi et al., 2008; Wang et al., 2006; Zhang et al., 2010). While the pollution issues vary among regions to a degree, we think that it is important to investigate typical pollution levels and characterize the chemical characteristics of the fine particles from across the Guanzhong Plain.

From the present study, we collected $PM_{2.5}$ samples at six monitoring sites in three major cities on the Guanzhong Plain and a reference site over the course of a year. The objectives of the study were to (1) characterize the $PM_{2.5}$ mass loadings and the concentrations of selected chemicals in airborne particles from each of the four seasons; (2) investigate the spatial and temporal variations of $PM_{2.5}$, (3) identify and assess the contributions of the potential sources for $PM_{2.5}$; and (4) obtain information through model simulations that will be useful for the development of the pollutant control strategies needed to attain the national standards.

2. Methdology

2.1. Sampling sites

A total of six sampling sites were used for this study, including three in Xi'an, one in Weinan, one in Baoji, and one in the Qinling Mountains. The locations are shown in Fig. 1. Detailed descriptions of the sampling sites are as follows:

(i) Xi'an High-Tech Zone (HT). This site was located in an urban zone ~15 km southwest of the downtown, and it was mostly surrounded by residential areas. There were no major industrial activities or local fugitive dust sources around the site. The air sampler was set up ~10 m above the ground level on the rooftop of the main building of the Institute of Earth Environment, Chinese Academy of Sciences.

(ii) Xi'an Jiaotong University (XJ). Located southeast of the downtown area and ~100 m from the South Second Ring Road, this site was affected by heavy traffic. The university's campus and residential units were to its north and east while several major roads were to the south and west. The sampler was placed on the rooftop of an 18-m tall building inside the campus.

(iii) Xi'an North Third Ring (NR). This site was to the north of a suburban region and within the Wei Shui Campus of Chang'an University. The campus is ~200 m away from a high-speed railway, 500 m to the east of the airport highway, and 1 km from the North Third Ring where the daily traffic is heavy. The sampler was setup on the rooftop of a 15-m tall building.

(iv) Weinan (WN). The site was located in the center of Weinan city, and there are chemical fertilizer factories and thermal power plants close to the downtown area. The sampler was installed 10 m above ground level on the rooftop of the Weinan Municipal Environmental Protection Bureau.

(v) Baoji (BJ). The site is to the east of Baoji city and next to a commercial center where there is heavy traffic but no industries are nearby. The sampler was set up 10 m above the ground level on the rooftop of the Baoji Municipal Environmental Protection Bureau.

(vi) Qinling Mountains (QM). Located 20 km south of Xi'an city, QM was defined as a background site; however, as a result of the prevailing northeasterly winds, the air quality on the Guanzhong Plain is nearly always impacted by emissions from Xi'an and other nearby cities. The QM site was on the Cuihua Mountains at an altitude of ~1200 m, and the sampler was placed 3 m above ground level.

2.2. Sample collection

Twenty-four hour $PM_{2.5}$ samples were collected from March 2012 to March 2013, and they were grouped by the four seasons as follows: spring (March to May), summer (June to August), autumn (September to November), and winter (December to February). A total of 527 samples were collected with mini-volume samplers (Airmetrics, Oregon, USA) that operated at a flow rate of 5 L min^{-1}. The sampling was conducted every 3 day at HT (124 samples), XJ (124 samples), and NR (124 samples), while at WN (63 samples) and BJ (64 samples), the samples were collected every six days; and at QM (28 samples), the samples were collected every 12 days. The $PM_{2.5}$ samples were collected on 47-mm quartz fiber filters (Whatman QM/A, Maidstone, UK), that were pre-combusted at 900 °C for 3 h. To minimize the evaporation of volatile components, each loaded sample filter was placed in a clean polystyrene petri dish and stored in a refrigerator at <4 °C prior to analysis.

A gravimetric method was used for determination of aerosol mass concentrations. For this method, each filter was equilibrated at a controlled temperature (20–23 °C) and relative humidity (RH, 35–45%) for 24 h prior to and after sampling. The filters were

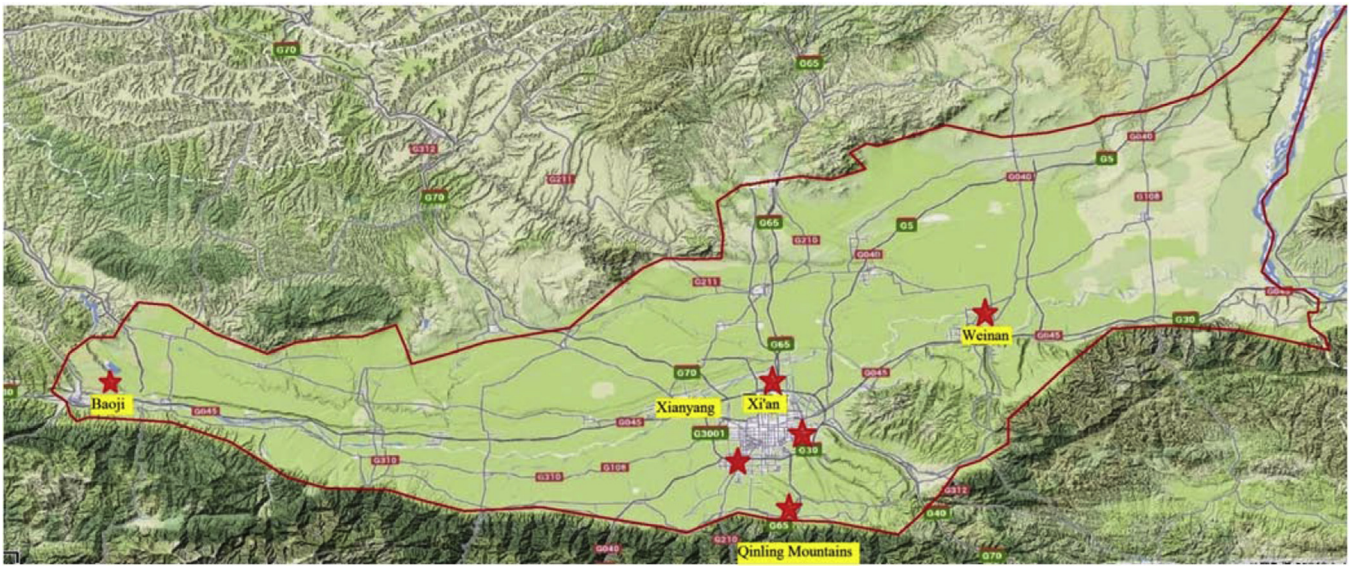

Fig. 1. Locations of six sampling sites in Guanzhong Plain.

weighed twice on an M5 electronic microbalance (±1 μg sensitivity, Sartorius, Gottingen, Germany). The precision was <15 μg per filter before sampling and <20 μg after sampling, and reweighing was required when the weight difference between replicates was greater than these respective values.

2.3. Chemical analysis

Organic carbon (OC) and elemental carbon (EC) were determined for 0.5 cm^2 punches prepared from each of the sample filter. A DRI model 2001 carbon analyzer (Atmoslytic, Inc., Calabasas, CA, USA) was used for these determinations following the IMPROVE_A thermal/optical reflectance (TOR) protocol (Cao et al., 2003; Chow et al., 1993). The sample aliquot was heated in a series of steps to determine the concentrations of four OC fractions (OC1, OC2, OC3, and OC4) in a helium atmosphere and OP (pyrolyzed carbon fraction) and three EC fractions (EC1, EC2, and EC3) in a 2% O_2/98% He atmosphere. The analyzer was calibrated with known quantities of methane (CH_4) each day of use. The IMPROVE protocol defined OC as OC1 + OC2 + OC3 + OC4 + OP and EC as EC1 + EC2 + EC3 − OP. Replicate analyses were performed at a frequency of one per group of 10 samples. The relative deviation of replicate analysis was <5% for TC (total carbon, the sum of OC and EC), and <10% for OC and EC.

The concentrations of five cations (Na^+, NH_4^+, K^+, Mg^{2+}, Ca^{2+}) and four anions (F^-, Cl^-, NO_3^-, SO_4^{2-}) were determined in aqueous extracts of the $PM_{2.5}$ samples (Zhang et al., 2011) with the use of a Dionex-600 Ion Chromatograph (Dionex Inc., Sunnyvale, CA, USA). The details for the sample extraction procedures have been presented elsewhere (Zhang et al., 2011). An IonPac AS14A column (8 mM Na_2CO_3/1 mM $NaHCO_3$ as the eluent) and an IonPacCS12A column (20 mM methanesulfonic acid as the eluent) were used for the separation of cations and anions respectively. The minimum detection limits (MDLs in mg L^{-1}) for the ions were: 4.6 for Na^+, 4.0 for NH_4^+, 10.0 for K^+, Mg^{2+} and Ca^{2+}, 0.5 for F^-,Cl^- and Br^-,15 for NO_2^- and NO_3^-, and 20 for SO_4^{2-}. The concentrations were corrected for sampling artifacts by subtracting the field blanks from the sample concentrations.

Energy Dispersive X-Ray Fluorescence (ED-XRF) spectrometry (Epsilon 5 ED-XRF, PANalytical B. V., Netherlands) was used to determine the concentrations of selected elements on the $PM_{2.5}$ quartz fiber filters (Steinhoff et al., 2000; Xu et al., 2012). Each sample was analyzed for 30 min to obtain a spectrum of X-ray counts versus photon energies, in which the individual peak energies matched specific elements, and the peak areas varied with elemental concentrations. Laboratory filter blanks also were analyzed to evaluate analytical bias. The elements that were determined by the EDXRF method include Mn, Ti, Fe, Zn, As, Br and Pb; the MLDs for these elements were 0.014, 0.005, 0.011, 0.008, <0.001, 0.006 and 0.015 μg cm^{-2}, respectively.

2.4. Coefficient of divergence

The coefficient of divergence (CD) for the mean $PM_{2.5}$ chemical compositions concentrations at two sampling sites can be used to assess the extent of uniformity within a given area (Wongphatarakul et al., 1998). The CD is a self-normalized parameter that is calculated as follows:

$$CD_{jk} = \sqrt{\frac{1}{p}\sum_{i=1}^{p}\left(\frac{X_{ij} - X_{jk}}{X_{ij} + X_{jk}}\right)^2} \quad (1)$$

where X_{ij} represents the average concentration for a chemical component i at site j, j and k represent the two sampling sites, and p is the number of the chemical species. For this statistic, CD approaches zero when the two sampling sites are similar and approaches unity when they are very different (Wongphatarakul et al., 1998).

2.5. Box model

A box model was used to calculate the atmospheric capacity (k ton yr^{-1}) for the Guanzhong Plain annually and for each season. The results of those calculations were then used to calculate the maximum air pollution emissions for each of the four seasons that would keep the pollutant loadings below the 35 μg m^{-3} mandated by the proposed air-quality standards. According to the principle of mass conservation, the $PM_{2.5}$ concentrations in the box model should be closely correlated to the ground-level emissions, production by chemical reactions, vertical diffusion, sedimentation, and advection of the particles into the box. The factors that would

affect the $PM_{2.5}$ concentrations in the box model can be written as follows:

$$\frac{\partial[X]}{\partial t} = \frac{\partial[X]_E}{\partial t} + \frac{\partial[X]_T}{\partial t} + \frac{\partial[X]_V}{\partial t} + \frac{\partial[X]_C}{\partial t} + \frac{\partial[X]_D}{\partial t} \quad (2)$$

where $\partial[X]/\partial t$ is the local variation of $PM_{2.5}$ concentrations; $[X]_E$ is the emissions at ground level; $[X]_T$ is the advection; $[X]_V$ is the vertical diffusions; $[X]_C$ is production by chemical reactions; and $[X]_D$ is sedimentation.

For the modeling studies, the Guanzhong area was defined as a long, narrow box as shown in Supplementary Fig. S1, and several assumptions were made in the calculations of the permissible capacity of atmosphere: (1) the SIA was generated through gas-particle chemical conversion processes; (2) pollutants within the boundary layer were homogeneously mixed, and the exchange between the boundary layer and other layers of the atmosphere were ignored; (3) the sedimentation of fine particles, which is typically slow (Han et al., 2016) was ignored, and (4) only east-west horizontal diffusion was considered because the north/south transport pathways were blocked by the Qinling Mountains to the north and Loess Plateau to the south. The capacity of pollutant emissions for the region was thus calculated as follows:

$$EMIS = WS \times ([X]_{out} - [X]_{in}) \times PBLH/DL \quad (3)$$

where EMIS is the total pollutant emissions to the Guanzhong Plain in kilotons per year – including primary particles and SIA precursors (i.e., SO_2 and NO_x) – that would keep the $PM_{2.5}$ loadings below permissible levels; PBLH is the atmospheric boundary-layer height; WS is the horizontal wind velocity; $[X]_{in}$ is the input $PM_{2.5}$ concentrations in the upper boundary; $[X]_{out}$ is output of $PM_{2.5}$ through the leeward boundary; and DL is the regional boundary length.

2.6. Weather research and forecasting chemical model

A regional dynamical/chemical transport model (Weather Research and Forecasting Chemical model—WRF-Chem) was used to simulate the effects of emission controls on the $PM_{2.5}$ concentrations over the Guanzhong Plain. The model as used in this study included on-line calculations of dynamical inputs (winds, temperature, planetary boundary layer etc.), transport (advective, convective and diffusive), dry deposition (Wesely, 1989), wet deposition, and surface emissions.

The model resolution was 6 × 6 km, the latitude and longitude of the model's central point were 119.00°E,34.25°N, and the model consisted of twenty-eight vertical layers from the surface to 50 hPa. The meteorological initial and boundary conditions were obtained from the NCEP 1° × 1° reanalysis data; and the initial and boundary condition were calculated from the 6 h output of a global chemistry transport model—MOZART4 (Model for OZone And Related chemical Tracers, Version 4). In the model, the Lin microphysics scheme (Lin et al., 1983), the Yonsei University (YSU) planetary boundary layer scheme (Noh et al., 2003), and Noah land-surface model (Chen and Dudhia, 2001) were employed. The Mlawer scheme (Mlawer et al., 1997) was used for the long-wave radiation parameterization and the Dudhia scheme (Dudhia, 1989) was used in the shortwave radiation parameterization.

3. Results and discussion

3.1. $PM_{2.5}$ mass and chemical compositions

Table 1 summarizes the annual and seasonally averaged $PM_{2.5}$ mass concentrations for each of the six sampling sites. The 24-h average $PM_{2.5}$ mass concentrations at the six sites varied from 24.0 to 535.2 μg m^{-3}, and the grand arithmetic mean concentration was 134.7 μg m^{-3}, which is far higher than the levels associated with health concerns. For comparison, the Chinese Class II $PM_{2.5}$ Standard for the annual average $PM_{2.5}$ mass concentration is 35 μg m^{-3}. Standard deviations (SD) for the mass loadings typically ranged from 25% to 50% of the means, indicating the samples were not greatly influenced by exceptional events during the study. Of the six sampling sites, those in Xi'an (HT, XJ and NR) showed the highest annual average concentration of 134.7 μg m^{-3}; this was 8.4% higher than WN (124.3 μg m^{-3}) and 9.5% higher than BJ (123.1 μg m^{-3}).

The background site of QM had the lowest annual $PM_{2.5}$ mass concentration (105.6 μg m^{-3}), but even there, the level there was still more than three times the air quality standard in China, and this illustrates the pervasive impacts of pollutant outflow from Xi'an and surrounding areas to QM under the prevailing north-easterly winds. Fig. 2 illustrates the temporal variations of the $PM_{2.5}$ mass at the six sampling sites, all of which showed the highest loadings in winter and the lowest in summer. The seasonal variations also showed general similarities throughout the Guanzhong Plain.

The grand average OC and EC mass concentrations in $PM_{2.5}$ were 24.5 and 5.6 μg m^{-3}, respectively. All six sites showed the highest OC and EC loadings in winter and the lowest values in summer (Table 1). The EC levels often varied with OC, but the variance in OC was greater than that of EC: this we ascribed to more stable emissions of EC. In this regard, OC can be generated from both primary sources (emitted directly from combustion and other processes) as well as secondary sources (generated by gas-to-particle conversion) (Cao et al., 2003; Ho et al., 2003), and this can lead to greater variability in the OC particles compared with EC.

The three most abundant inorganic ions in the PM in order were SO_4^{2-}, NO_3^- and NH_4^+ (Table 1). The sum of SO_4^{2-} and NO_3^- accounted for over 65% of the total quantified ions and NH_4^+ had a stable contribution of 15–17% among the sites. Ammonia can react with sulfuric acid or sulfate to produce ammonium sulfate ($(NH_4)_2SO_4$), and gas-phase reactions between ammonia and nitric acid can generate ammonium nitrate (NH_4NO_3) (Kerminen et al., 2001; Cheng et al., 2011; Han et al., 2016). The likely contributions of those reactions attest to the importance of reducing both precursor gases and primary PM emissions for $PM_{2.5}$ control. Increased photochemical activity is one of the possible reasons for the enhanced sulfate and secondary ion production in summer. On the other hand, the relatively low ambient temperatures and the high emissions of NO_x in winter would favor (1) the conversion of gaseous nitric acid into aerosol particles or filterable NO_3^- and (2) gas-particle reactions that convert gaseous NH_3 to aerosol NH_4^+ (Cao et al., 2009).

Three elements (Ti, Fe and Mn) are often used as crustal markers due to their well-established concentrations in mineral matter and their generally low chemical reactivity in most geological materials (Duan et al., 2006; Cao et al., 2012a). High concentrations of these and other crustal elements were found at the sites in Xi'an, especially NR, where the mineral dust contribution to the $PM_{2.5}$ mass was especially large (Table 1). The large peaks in Ti, Fe and Mn always occurred in spring which is when dust storms are common (Shen et al., 2007). Various other elements, including As and Pb are enriched in coal, and their concentrations are commonly above natural levels in the atmosphere because of the emissions from coal burning. Impacts from this sources are consistent with the finding that the highest levels of the elements and other pollutants occurred in winter because that is when large quantities of coal are burned for domestic heating (Okuda et al., 2010; Shen et al., 2010; Cao et al., 2008b).

Table 1
Arithmetic averages of $PM_{2.5}$ mass and chemical components of the $PM_{2.5}$ in Guanzhong Plain (unit: μg m^{-3}).

Sites	Xi'an High-Tech Zone					Xi'an Jiaotong University					Xi'an North Third Ring				
	Spring	Summer	Autumn	Winter	Yearly	Spring	Summer	Autumn	Winter	Yearly	Spring	Summer	Autumn	Winter	Yearly
$PM_{2.5}$	151.7 ± 56.6	108.3 ± 40.5	160.7 ± 89.3	263.4 ± 132.9	169.3 ± 101.7	156.7 ± 49.5	90.7 ± 30.8	127.9 ± 66.4	222.6 ± 114.3	149.1 ± 85.6	183.9 ± 67.0	126.8 ± 44.5	176.8 ± 84.3	245.5 ± 105.2	184.3 ± 89.6
OC	22.4 ± 7.9	15.6 ± 14.8	29.0 ± 15.4	36.2 ± 19.2	28.6 ± 20.0	22.4 ± 7.9	15.6 ± 14.8	29.0 ± 15.4	36.2 ± 19.2	25.5 ± 16.4	23.1 ± 9.7	13.0 ± 6.7	34.2 ± 21.8	46.8 ± 28.9	29.2 ± 22.8
EC	5.7 ± 2.5	3.6 ± 2.4	8.2 ± 3.9	7.8 ± 3.9	7.1 ± 5.4	5.7 ± 2.5	3.6 ± 2.4	8.2 ± 3.9	7.8 ± 3.9	6.3 ± 3.7	6.9 ± 3.3	4.7 ± 2.1	9.3 ± 5.6	10.0 ± 5.1	7.7 ± 4.7
Na^+	1.6 ± 0.7	1.0 ± 0.6	0.9 ± 1.5	2.8 ± 1.2	1.7 ± 1.2	1.8 ± 0.7	1.7 ± 1.1	0.7 ± 0.5	2.21.0	1.6 ± 1.0	1.2 ± 0.4	1.5 ± 0.4	0.4 ± 0.3	1.0 ± 1.0	1.1 ± 0.7
NH_4^+	7.5 ± 5.9	7.2 ± 5.7	7.9 ± 5.9	17.1 ± 12.1	9.6 ± 8.7	5.6 ± 5.6	6.0 ± 5.1	8.5 ± 6.4	17.5 ± 10.5	9.1 ± 8.6	6.3 ± 5.2	6.5 ± 5.5	8.3 ± 6.3	15.8 ± 9.1	9.2 ± 7.7
K^+	0.9 ± 0.7	0.6 ± 0.5	1.2 ± 0.9	2.8 ± 1.9	1.3 ± 1.4	0.9 ± 0.6	0.9 ± 0.4	1.5 ± 0.9	3.2 ± 3.1	1.5 ± 1.8	1.0 ± 0.6	1.0 ± 0.6	1.7 ± 1.0	2.8 ± 1.6	1.6 ± 1.3
Mg^{2+}	0.3 ± 0.2	0.1 ± 0.1	0.2 ± 0.2	0.5 ± 0.2	0.3 ± 0.2	0.3 ± 0.2	0.2 ± 0.1	0.1 ± 0.1	0.6 ± 0.4	0.3 ± 0.3	0.4 ± 0.3	0.2 ± 0.1	0.2 ± 0.1	0.7 ± 0.3	0.4 ± 0.3
Ca^{2+}	3.4 ± 1.9	2.1 ± 1.1	1.7 ± 1.6	2.5 ± 1.6	2.5 ± 1.7	3.6 ± 2.0	2.2 ± 1.5	1.6 ± 1.3	2.2 ± 1.4	2.5 ± 1.7	4.5 ± 2.9	1.8 ± 1.0	2.1 ± 1.9	2.5 ± 2.2	2.8 ± 2.4
F^-	0.2 ± 0.1	0.03 ± 0.03	0.2 ± 0.3	0.6 ± 0.4	0.3 ± 0.3	0.2 ± 0.1	0.2 ± 0.1	0.3 ± 0.2	0.5 ± 0.4	0.3 ± 0.2	0.2 ± 0.1	0.1 ± 0.1	0.3 ± 0.2	0.4 ± 0.3	0.2 ± 0.2
Cl^-	3.0 ± 1.8	0.6 ± 0.4	3.3 ± 3.5	8.4 ± 4.7	3.8 ± 4.1	2.6 ± 1.4	0.8 ± 0.6	4.3 ± 3.7	8.5 ± 5.2	3.9 ± 4.5	3.1 ± 2.0	1.5 ± 1.1	5.4 ± 4.4	8.1 ± 5.4	4.5 ± 4.4
NO_3^-	16.1 ± 13.1	9.8 ± 8.9	15.3 ± 13.2	29.2 ± 25.3	17.1 ± 17.3	14.2 ± 11.7	9.4 ± 8.0	16.8 ± 13.5	30.4 ± 20.2	17.2 ± 15.7	15.4 ± 11.5	11.0 ± 8.2	17.3 ± 12.7	28.3 ± 18.7	17.8 ± 14.7
SO_4^{2-}	18.4 ± 11.2	23.4 ± 13.4	17.3 ± 11.5	31.7 ± 25.1	22.2 ± 16.8	17.0 ± 10.7	23.7 ± 14.0	18.8 ± 11.5	34.2 ± 20.7	22.8 ± 15.6	18.0 ± 9.7	27.8 ± 15.4	19.9 ± 13.4	30.4 ± 17.4	23.7 ± 15.0
Ti	0.21 ± 0.16	0.05 ± 0.05	0.10 ± 0.08	0.10 ± 0.05	0.11 ± 0.11	0.23 ± 0.15	0.07 ± 0.06	0.08 ± 0.05	0.10 ± 0.06	0.12 ± 0.11	0.27 ± 0.19	0.08 ± 0.07	0.13 ± 0.10	0.13 ± 0.10	0.15 ± 0.14
Mn	0.13 ± 0.06	0.04 ± 0.02	0.11 ± 0.07	0.11 ± 0.07	0.10 ± 0.07	0.11 ± 0.05	0.03 ± 0.02	0.07 ± 0.04	0.10 ± 0.06	0.08 ± 0.05	0.15 ± 0.08	0.06 ± 0.04	0.14 ± 0.10	0.12 ± 0.08	0.11 ± 0.08
Fe	2.53 ± 1.73	0.70 ± 0.49	1.34 ± 1.06	1.41 ± 0.75	1.48 ± 1.27	2.77 ± 1.70	0.84 ± 0.53	1.06 ± 0.62	1.37 ± 0.84	1.54 ± 1.29	3.32 ± 2.26	1.12 ± 0.73	1.86 ± 1.35	1.77 ± 1.22	1.98 ± 1.65
Zn	1.61 ± 1.30	0.61 ± 0.45	2.03 ± 1.50	1.86 ± 1.45	1.52 ± 1.35	2.12 ± 1.60	0.44 ± 0.24	1.05 ± 0.63	1.18 ± 0.96	1.21 ± 1.17	1.73 ± 1.55	1.05 ± 1.05	3.19 ± 3.38	2.13 ± 2.31	2.02 ± 2.37
As	0.03 ± 0.02	0.02 ± 0.02	0.03 ± 0.02	0.04 ± 0.04	0.03 ± 0.03	0.02 ± 0.01	0.02 ± 0.02	0.03 ± 0.02	0.04 ± 0.04	0.03 ± 0.03	0.02 ± 0.02	0.02 ± 0.02	0.02 ± 0.02	0.06 ± 0.05	0.03 ± 0.03
Br	0.03 ± 0.02	0.01 ± 0.01	0.05 ± 0.04	0.06 ± 0.04	0.03 ± 0.03	0.03 ± 0.02	0.01 ± 0.01	0.04 ± 0.03	0.05 ± 0.03	0.03 ± 0.03	0.04 ± 0.02	0.01 ± 0.01	0.06 ± 0.05	0.05 ± 0.03	0.04 ± 0.03
Pb	0.22 ± 0.10	0.12 ± 0.07	0.31 ± 0.20	0.41 ± 0.30	0.26 ± 0.22	0.29 ± 0.17	0.11 ± 0.06	0.22 ± 0.13	0.40 ± 0.28	0.25 ± 0.21	0.23 ± 0.12	0.17 ± 0.05	0.38 ± 0.26	0.39 ± 0.20	0.29 ± 0.20
Sites	Weinan					Baoji					Qinling Mountains				
	Spring	Summer	Autumn	Winter	Yearly	Spring	Summer	Autumn	Winter	Yearly	Spring	Summer	Autumn	Winter	Yearly
$PM_{2.5}$	118.5 ± 34.0	102.8 ± 33.6	126.9 ± 83.5	196.2 ± 80.0	135.5 ± 70.0	128.0 ± 54.3	89.2 ± 46.9	105.5 ± 59.4	204.7 ± 98.2	132.0 ± 78.5	79.0 ± 31.0	66.4 ± 20.2	114.6 ± 70.3	215.2 ± 93.0	120.3 ± 83.8
OC	17.2 ± 6.0	12.5 ± 5.6	23.0 ± 14.8	28.9 ± 9.5	20.2 ± 11.2	19.6 ± 7.0	10.5 ± 1.6	20.4 ± 12.0	43.5 ± 16.8	23.3 ± 15.9	10.6 ± 4.1	7.9 ± 2.2	19.5 ± 14.6	39.6 ± 14.8	20.1 ± 16.6
EC	3.8 ± 1.6	2.9 ± 1.3	5.0 ± 2.9	7.1 ± 2.6	4.6 ± 2.7	3.4 ± 1.5	3.3 ± 1.2	5.1 ± 3.0	6.2 ± 2.1	4.4 ± 2.3	1.6 ± 0.8	1.4 ± 0.5	3.8 ± 2.8	5.8 ± 3.4	3.2 ± 2.9
Na^+	1.4 ± 0.7	1.4 ± 0.6	0.5 ± 0.3	1.5 ± 0.8	1.3 ± 0.7	1.3 ± 0.8	1.0 ± 0.5	0.9 ± 0.6	1.6 ± 0.7	1.2 ± 0.7	1.8 ± 1.1	0.8 ± 0.4	0.9 ± 1.4	3.0 ± 0.9	1.5 ± 1.3
NH_4^+	5.6 ± 5.0	7.0 ± 5.1	10.7 ± 9.7	18.3 ± 10.1	10.0 ± 9.1	4.7 ± 5.6	7.0 ± 7.3	5.4 ± 5.1	14.2 ± 11.4	7.5 ± 8.3	1.2 ± 0.8	3.6 ± 2.9	7.8 ± 6.8	20.2 ± 7.6	7.2 ± 8.7
K^+	0.8 ± 0.6	0.9 ± 0.6	1.2 ± 1.0	2.6 ± 1.8	1.3 ± 1.3	0.6 ± 0.3	0.7 ± 0.5	0.7 ± 0.7	1.8 ± 1.5	0.9 ± 1.0	0.4 ± 0.3	0.5 ± 0.3	1.0 ± 0.9	2.8 ± 1.5	1.0 ± 1.3
Mg^{2+}	0.2 ± 0.1	0.1 ± 0.1	0.1 ± 0.1	0.3 ± 0.2	0.2 ± 0.1	0.2 ± 0.2	0.1 ± 0.1	0.1 ± 0.1	0.4 ± 0.1	0.2 ± 0.2	0.2 ± 0.1	0.1 ± 0.0	0.1 ± 0.2	0.5 ± 0.1	0.2 ± 0.2
Ca^{2+}	2.1 ± 1.4	0.8 ± 0.5	1.2 ± 0.9	1.1 ± 0.7	1.6 ± 1.0	1.7 ± 0.8	0.8 ± 0.5	1.1 ± 0.7	1.6 ± 1.0	1.3 ± 0.8	1.7 ± 1.0	0.5 ± 0.4	0.7 ± 1.2	1.8 ± 0.6	1.1 ± 1.0
F^-	0.1 ± 0.1	0.1 ± 0.1	0.1 ± 0.1	0.3 ± 0.2	0.1 ± 0.1	0.1 ± 0.1	0.1 ± 0.0	0.1 ± 0.1	0.2 ± 0.2	0.1 ± 0.1	0.2 ± 0.1	0.1 ± 0.1	0.1 ± 0.2	0.5 ± 0.2	0.2 ± 0.2
Cl^-	1.8 ± 1.0	0.9 ± 0.4	3.0 ± 2.0	6.9 ± 3.6	3.0 ± 3.1	1.8 ± 1.1	1.0 ± 0.6	2.2 ± 2.0	4.5 ± 1.8	2.3 ± 1.9	0.7 ± 0.3	0.4 ± 0.1	1.3 ± 1.3	5.4 ± 3.0	1.7 ± 2.5
NO_3^-	12.2 ± 10.4	9.9 ± 8.0	21.0 ± 20.0	31.5 ± 20.7	18.0 ± 17.5	10.8 ± 11.8	10.5 ± 11.3	12.0 ± 10.1	28.6 ± 27.2	14.8 ± 17.7	7.1 ± 5.5	5.5 ± 5.7	18.6 ± 17.9	33.0 ± 12.1	14.8 ± 15.6
SO_4^{2-}	18.4 ± 10.9	28.5 ± 13.3	21.3 ± 17.4	34.1 ± 21.1	24.7 ± 16.8	15.0 ± 11.0	25.2 ± 19.2	13.5 ± 8.5	28.7 ± 20.2	19.8 ± 16.3	11.6 ± 6.6	18.5 ± 8.5	17.3 ± 10.2	37.6 ± 14.9	19.3 ± 13.6
Ti	0.10 ± 0.06	0.03 ± 0.03	0.03 ± 0.03	0.04 ± 0.02	0.05 ± 0.05	0.15 ± 0.12	0.02 ± 0.02	0.08 ± 0.07	0.12 ± 0.06	0.10 ± 0.09	0.09 ± 0.03	0.01 ± 0.01	0.04 ± 0.02	0.05 ± 0.01	0.04 ± 0.03
Mn	0.03 ± 0.03	0.02 ± 0.01	0.01 ± 0.01	0.05 ± 0.03	0.03 ± 0.03	0.11 ± 0.06	0.05 ± 0.04	0.06 ± 0.06	0.14 ± 0.20	0.09 ± 0.11	0.04 ± 0.03	0.01 ± 0.00	0.01 ± 0.01	0.04 ± 0.03	0.02 ± 0.02
Fe	1.12 ± 0.74	0.56 ± 0.24	0.56 ± 0.26	0.80 ± 0.32	0.77 ± 0.50	1.87 ± 1.46	0.60 ± 0.14	1.09 ± 0.81	1.14 ± 0.52	1.22 ± 1.02	0.95 ± 0.38	0.27 ± 0.11	0.43 ± 0.31	0.86 ± 0.32	0.62 ± 0.40
Zn	0.49 ± 0.28	0.26 ± 0.17	0.43 ± 0.27	0.61 ± 0.41	0.45 ± 0.31	1.51 ± 0.89	1.28 ± 0.76	1.59 ± 1.07	1.35 ± 0.78	1.44 ± 0.87	0.21 ± 0.17	0.15 ± 0.12	0.34 ± 0.36	0.52 ± 0.56	0.31 ± 0.37
As	0.03 ± 0.04	0.03 ± 0.03	0.05 ± 0.03	0.08 ± 0.05	0.05 ± 0.04	0.04 ± 0.02	0.04 ± 0.03	0.03 ± 0.01	0.07 ± 0.05	0.05 ± 0.03	0.01 ± 0.00	0.00 ± 0.00	0.03 ± 0.02	0.05 ± 0.02	0.03 ± 0.02
Br	0.02 ± 0.01	0.01 ± 0.01	0.04 ± 0.02	0.04 ± 0.02	0.03 ± 0.02	0.02 ± 0.01	0.01 ± 0.01	0.03 ± 0.03	0.03 ± 0.02	0.03 ± 0.02	0.01 ± 0.00	0.00 ± 0.00	0.02 ± 0.01	0.03 ± 0.02	0.02 ± 0.02
Pb	0.15 ± 0.09	0.14 ± 0.08	0.20 ± 0.10	0.32 ± 0.15	0.20 ± 0.13	0.02 ± 0.01	0.02 ± 0.01	0.04 ± 0.06	0.02 ± 0.01	0.02 ± 0.03	0.07 ± 0.04	0.05 ± 0.03	0.12 ± 0.09	0.30 ± 0.18	0.14 ± 0.14

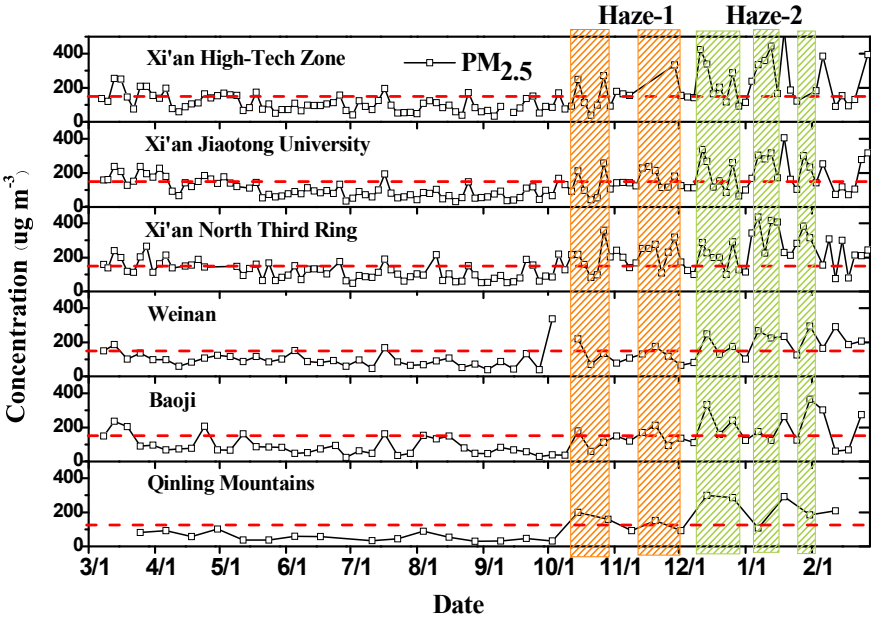

Fig. 2. Time series of $PM_{2.5}$ mass concentrations at six sampling sites. The shaded areas show pollution episodes, the red line show the haze standard of 150 μg/m^3 based on the "Technical Regulation on Ambient Air Quality Index (on trial)". (For interpretation of the references to colour in this figure legend, the reader is referred to the web version of this article.)

The CD values of chemical components between the pairs of six sampling sites are shown in Supplementary Table S1. The calculated CD values for the pairs of sites in Xi'an were ~0.1 and lower while those between other pairs of sites were 0.2–0.3. The CD calculations also showed that the background site of QM was the least similar to other sites. These relatively low CD values indicate that the chemical composition of the $PM_{2.5}$ was relatively consistent over the spatial scale of the study.

3.2. Source identification

The ratios of OC/EC, SO_4^{2-}/OC, SO_4^{2-}/EC, NO_3^-/SO_4^{2-}, As/Fe, and Pb/Fe have been used as indicators of domestic and industrial coal use, and these ratios were calculated for our study sites and compared with the values found in various cities around the world (Table 2). The OC/EC ratio is commonly used as a measure of the impacts of fossil fuel emissions and aging, and especially the formation of secondary organic aerosols (Chow et al., 1993; Zeng and Wang, 2011). The average OC/EC ratio for our sites on the Guanzhong Plain (4.48 ± 1.72) was higher than those in several other cities, especially in winter when the average OC/EC ratio was as high as 5.80 in our study area. These high ratios can be explained by strong influences from biomass and coal combustion combined with the aging of emissions in the atmosphere (Koch, 2001; Cao et al., 2005), and it is worth mentioning that Chinese cities are typically more strongly influenced by combustion activities than those in most other countries. The SO_4^{2-}/OC and SO_4^{2-}/EC ratios in our study also were much higher than the other cities in the comparison, and that can be explained by the emissions of SO_4^{2-} from coal burning and the large quantities of secondary aerosols generated at our sites.

The NO_3^-/SO_4^{2-} ratio has been used to evaluate the relative contributions of stationary versus mobile sources for PM (Arimoto et al., 1996; Hu et al., 2002; Lai et al., 2007; Wang et al., 2005). Engine exhausts from gasoline- and diesel-powered vehicles are the primary mobile source for NO_x, but this accounts for little SO_2. In our study, the average NO_3^-/SO_4^{2-} ratios in summer and winter were 0.38 and 0.89, respectively. The major factor that drove these variations was most likely seasonal changes in the emissions from coal combustion, but other stationary sources especially power plants and other industrial sources, also may have been important, and their contributions cannot be neglected. In Guangzhou, where the influences from stationary sources were relatively small, the NO_3^-/SO_4^{2-} ratios were much higher than those in Beijing, Shanghai or Toronto, and nearly five times those in Mexico City and Seattle.

The As/Fe and Pb/Fe ratios have been used as indicators of fly ash from uncontrolled coal combustion (Cao et al., 2012a). The values of these ratios at our sites were similar to other Chinese cities such as Beijing, Shanghai and Guangzhou, but they were much higher than

Table 2
Comparison of the chemical component ratios from selected cities.

Ratio	City						
	Guanzhong Plain	Beijing, China	Shanghai, China	Guangzhou, China	Hong Kong, China	Mexico City, Mexico	Yokohama, Japan
OC/EC	4.48 ± 1.72	3.69	3.28	4.27	3.57	2.22	1.93
SO_4^{2-}/OC	1.25 ± 1.16	0.98	0.84	0.32	0.84	0.32	1.01
SO_4^{2-}/EC	5.22 ± 4.48	3.61	2.75	1.37	1.59	0.71	1.96
NO_3^-/SO_4^{2-}	0.76 ± 0.40	0.63	0.6	2.14	0.07	0.45	0.25
As/Fe	0.04 ± 0.04	0.03	0.04	0.02	–	0.006	–
Pb/Fe	0.23 ± 0.23	0.26	0.4	0.24	0.4	0.068	–
Reference	This study	(Cao et al., 2012a)	(Cao et al., 2012a)	(Yang et al., 2011)	(Cheng et al., 2010)	(Vega et al., 2004)	(Khan et al., 2010)

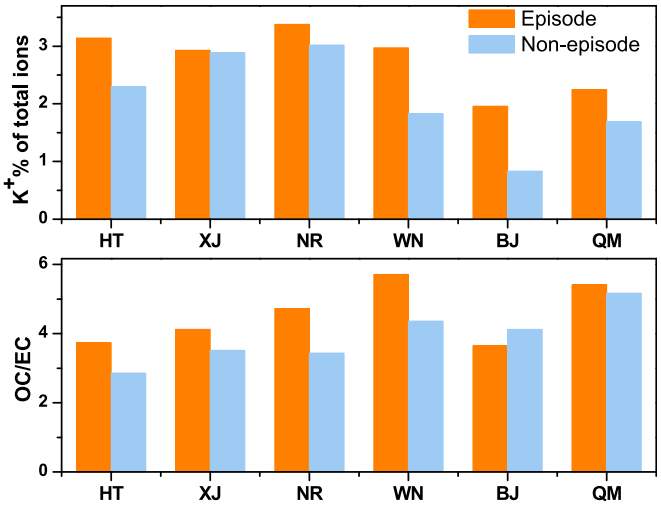

Fig. 3. Comparisons of K^+ contribution and OC/EC ratio in pollution and normal days during Haze-1.

those in Toronto, Mexico City and Seattle, indicating that there is still a pressing need for controls on coal fly-ash in China.

3.3. Pollution episode

Fig. 2 shows the dates for several pollution episodes, which were defined by daily concentrations of $PM_{2.5}$ > 150 μg m^{-3} (shown as red lines in Fig. 2), that occurred during our study. This criterion is based on the "Ambient Air Quality Standards" promulgated by the Chinese Ministry of Environmental Protection in 2012. Two heavily polluted periods occurred in autumn, from 15 to 27 October and 11–28 November. In winter, the high pollution levels tended to last much longer than those in other seasons: the two episodes during our study lasted from 11 to 26 December and 4–31 January. Based on their effects on visibility, we refer to the pollution periods in autumn and winter as "Haze-1" and "Haze-2", respectively in the following discussion. In the spring, a dust storm event occurred from 13 to 28 March, but that influence on the PM loadings in the study area was much less than that of pollution during haze events.

During Haze-1, the $PM_{2.5}$ mass loadings in Xi'an (i.e., HT, XJ, and NR) exceeded 200 μg m^{-3}, and the air pollution in that city was much more severe than at the other sites. Even so, the $PM_{2.5}$ variations were nearly synchronous across sites during the pollution episodes, demonstrating that the haze phenomena were likely a result of emissions from a complex set of regional sources. Soluble K^+ has been used as an indicator of biomass burning because it is strongly enriched in emissions from this source (Andreae, 1983; Chow et al., 2004; Duan et al., 2004). Fig. 3 compares the contributions of K^+ to the total quantified ions and the OC/EC ratios for the Haze-1 episode and non-episode days. The contribution of K^+ ranged from 2.0 to 3.4% of the total quantified ions, and the average was 32% higher than that for the non-episode days. This indicated that biomass burning was a major source for the regional pollution during Haze-1, and it was particularly important for the NR site.

The average ratio of OC/EC on the haze episode days was 16% higher than on the non-episode days, and this demonstrates the importance of secondary organic aerosols (SOAs) for the pollution events. Compared with fossil fuel combustion, carbonaceous aerosols emitted from biomass burning generally contain a relatively large proportion of OC, a typical OC/EC ratio for this source is 9.0 (Bond et al., 2004; Cachier et al., 1989). In contrast, relatively

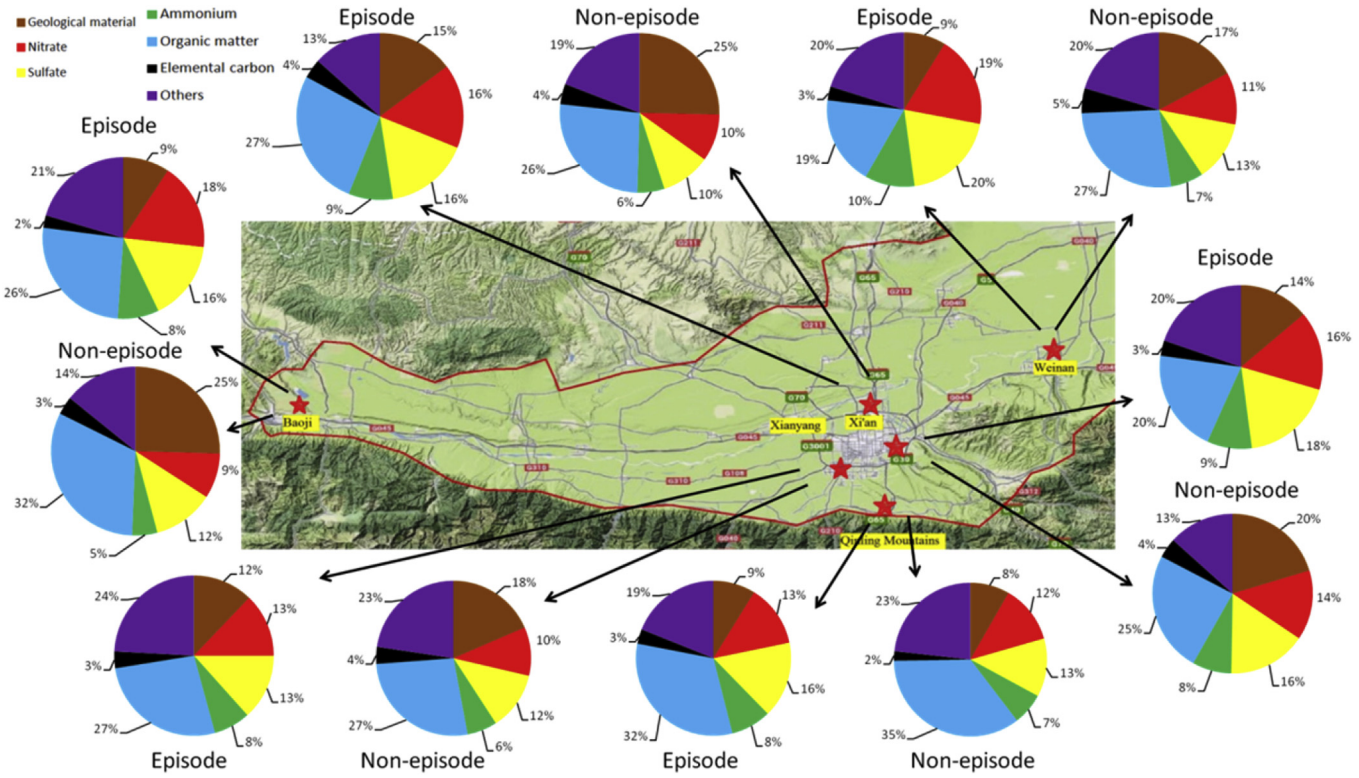

Fig. 4. Material balance of $PM_{2.5}$ for six sampling sites in episode and non-episode days during Haze-2. Organic matter (OM) is estimated as 1.6 × OC to account for unmeasured hydrogen and oxygen (El-Zanan et al., 2005; El-Zanan et al., 2009). Geological material is estimated as 25 × Fe to account for unmeasured oxygen and non-iron minerals (Cao et al., 2008a; Wu et al., 2011). "Others" is the remaining unaccounted-for mass after subtracting the sum of measured components from the $PM_{2.5}$ mass.

low OC/EC ratios (1.1 for motor vehicles) often are seen in areas that are greatly impacted by vehicular emissions (Watson et al., 2001). Hence, there are two lines of evidence – the elevated soluble K^+ and high OC/EC ratios – that point to strong impacts from biomass burning during the Haze-1 episode.

During the Haze-2 episode, the $PM_{2.5}$ mass concentrations were >300 μg m^{-3} at all three sites in Xi'an and exceeded 200 μg m^{-3} at WN, BJ and even the QM background site. Fig. 4 shows the material balances for $PM_{2.5}$ from the Haze-2 episode and non-episode days. Consistent with the previous discussion, organic material (OM) and secondary inorganic aerosols (SIA, i.e., SO_4^{2-}, NO_3^- and NH_4^+) were found to be the dominant components of the fine particles. The SIA contributed 10.4% more to the measured $PM_{2.5}$ mass on episode days (40.4%) compared with the non-episode days (30.0%). Extensive forests on the QM cover 48% of the land surface, and that vegetation can emit large quantities of VOCs that in turn can be oxidized to form particulate OC. Thus emissions of organic compounds from vegetation can explain the relatively high contribution of OM to the fine particles at our background site (Wang et al., 2015). Geological material (GM) also can be an important component of the aerosol, and iron often is used as a proxy for mineral dust because of its well-establish abundances in Chinese loess and soils (Cao et al., 2008a; Wu et al., 2011). The relative abundances of GM were the highest at the sites in Xi'an, and some of the mineral matter there was undoubtedly from fugitive dusts, which also have appreciable calcium contents. Overall, the ambient aerosol mass that was not accounted for by our chemical analysis was likely (a) unmeasured geological material, including calcium carbonate and some other minerals and (b) water associated with NH_4^+, NO_3^-, and SO_4^{2-} (Malm et al., 2011)

Our study shows that air pollution is a regional-scale problem for the Guanzhong Plain, and the results also show that the strategies for mitigating $PM_{2.5}$ pollution should focus not only on primary particulate emissions but also on secondary aerosol precursors, especially SO_2, NO_x, and NH_3. The SO_2 emissions and ambient sulfate $PM_{2.5}$ have shown an obvious decreasing trend beginning in 2006 due to the nationwide implementation of flue gas desulphurization controls (Wang et al., 2013). However, the SO_2 emissions that affect the Guanzhong Plain are still large, and it will be crucial to control and reduce SO_2 emissions further by

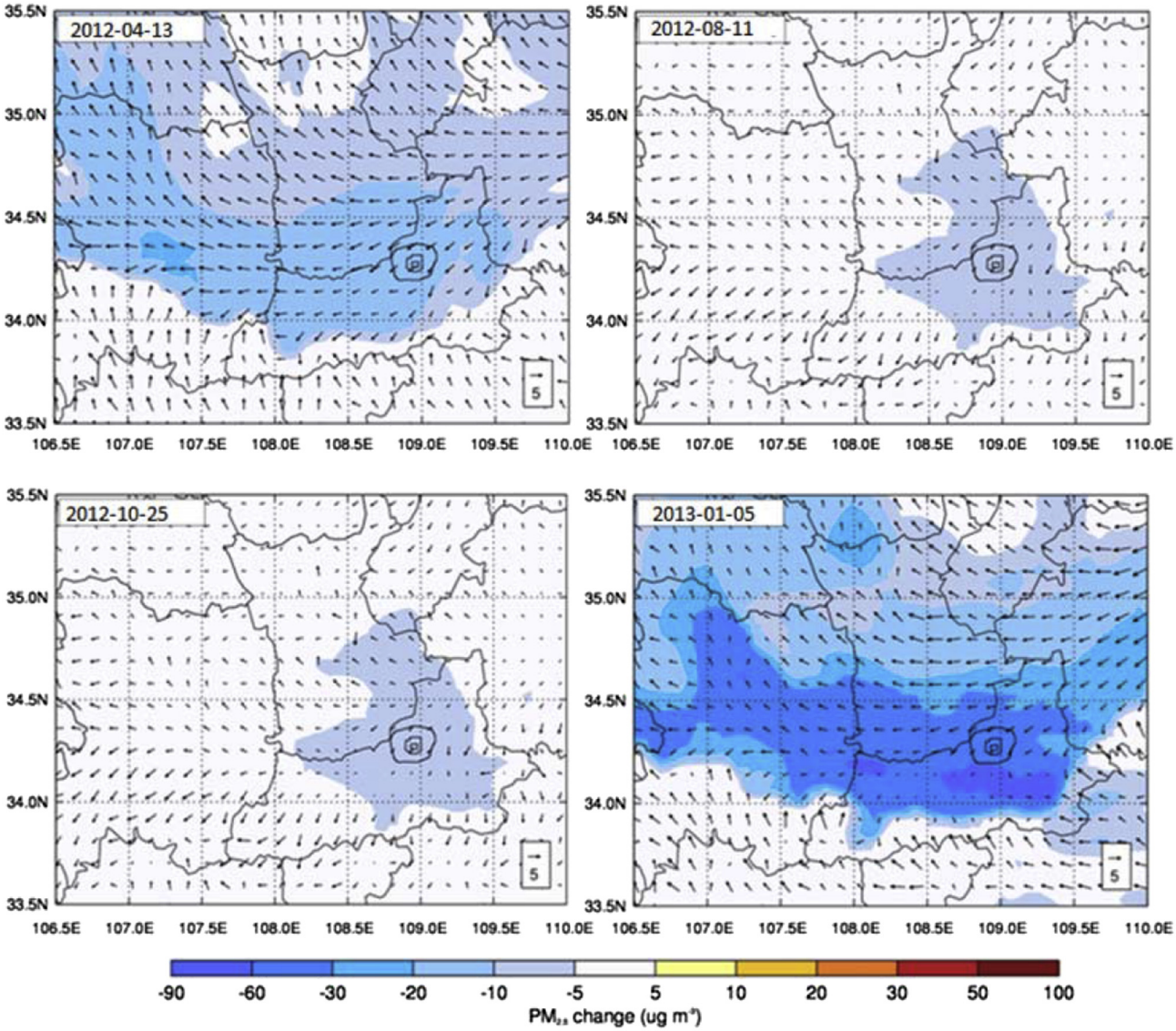

Fig. 5. Effects of strong emission reduction on $PM_{2.5}$ concentration.

developing advanced technologies for clean coal combustion, switching to low-sulfur fuels, continuing flue gas desulphurization controls, and effectively managing emissions from both coal-fired power plants and the boilers used for residential heating.

As a result of the lag between emission control legislation and an increase in fuel consumption by power plants and automobiles, the NO_x concentrations in China reached a peak in 2006 and then increased nearly 40% the following year (Huang et al., 2014). Improvements to denitrification technology could be an efficient means for controlling NO_x emissions from both industries and motor vehicle exhausts. We note, however, that NH_3 released from agriculture sources also can lead the formation of nitrate (and sulfate) in $PM_{2.5}$, but this has not been considered as an important air pollutant by the Chinese government. Effective controls on NH_3 emissions will require a combination of chemical, physical and biological methods, and these would need to be tailored to different environmental scenarios.

3.4. Atmospheric environment permissible capacity

Seasonally-adjusted parameters (see Supplementary Table S2) were used in the box model to compute a permissible atmosphere input capacity based on an assumed background $PM_{2.5}$ concentration of 20 μg m^{-3} and a more realistic target concentration of 75 μg m^{-3} that is the national standard. More representative atmosphere burdens were also calculated using seasonally matched ambient $PM_{2.5}$ concentrations (spring: 55.8 μg m^{-3},summer: 42.6 μg m^{-3},autumn: 75.1 μg m^{-3}, winter: 68.0 μg m^{-3}) along with seasonal data for methodological conditions. The permissible capacity decreased substantially from spring to winter while the capacity in spring was three times higher than that of winter (Table 3). This can be ascribed to the relatively low pollutant emissions in spring and meteorological conditions at that time of year that were favorable for the diffusion and transport of pollutants. The actual atmosphere capacity in autumn exceeded the maximum admissible emission, and there was almost no emission capacity in winter, indicating that emission reductions are most strongly needed in those two seasons.

3.5. Emission reduction assessments

Using the results from the box model, simulations of emission increases and reductions were made to assess the effects of changing emissions in the area. For each season, two days were selected as representative (spring: 12–13 April, summer: 10–11 August, autumn: 24–25 October, winter: 5–6 January); those were days when the pollutant levels were close to the seasonal averages. We assumed that four major sources were the main contributors to the $PM_{2.5}$ pollution and used these sources in our simulations; these were (i) industries, (ii) motor vehicles, (iii) residences and (iv) thermal power-plants. Variations in the $PM_{2.5}$ loadings were calculated for four different scenarios with the WRF-Chem model as follows: (S1) weak emission reduction, (S2) strong emission reduction, (S3) weak emission increasing, and (S4) strong emission increase. The details for each of these scenarios are given in Supplementary Table S3.

Table 3
Permissibleand actual atmospheric environment capacity in different seasons.

	Spring	Summer	Autumn	Winter
Permissibleatmosphere capacity (k·ton·yr^{-1})	179.8	97.6	81.6	42.3
Actual atmosphere capacity (k·ton·yr^{-1})	62.8	57.5	−0.2	5.4

Table 4
Results of $PM_{2.5}$ emission simulations in Guanzhong Plain.

Cities	Seasons	Emission Reduction		Emission Increase	
		Weak (S1)	Strong (S2)	Weak (S3)	Strong (S4)
Xi'an	Spring	−2.8%	−15.9%	11.2%	19.7%
	Summer	−6.3%	−19.9%	13.1%	21.0%
	Autumn	−13.3%	−30.4%	26.5%	39.8%
	Winter	−2.4%	−34.3%	20.0%	36.8%
	Average	−6.2%	−25.1%	17.7%	29.3%
Baoji	Spring	−4.6%	−16.7%	11.5%	19.0%
	Summer	−2.3%	−13.3%	7.0%	12.5%
	Autumn	−5.8%	−16.5%	14.4%	23.0%
	Winter	−2.2%	−35.1%	19.6%	37.0%
	Average	−3.7%	−20.4%	13.1%	22.9%
Weinan	Spring	−3.7%	−13.8%	9.6%	16.1%
	Summer	−5.5%	−16.2%	10.9%	17.0%
	Autumn	−11.3%	−28.4%	23.1%	35.4%
	Winter	−0.2%	−26.4%	15.6%	29.0%
	Average	−5.2%	−21.2%	14.8%	24.4%

The results of $PM_{2.5}$ emission simulations are shown in Table 4 and illustrated in Figs. 5 and 6. Under the moderate emission reduction scenario, the $PM_{2.5}$ mass concentration decreased by 6.2%, 3.7% and 5.2% in Xi'an, Baoji and Weinan, respectively, while with strong measures the decreases were as high as 25.1% in Xi'an. As shown in Fig. 6, under the strong emission reduction scenario, the most significant benefits would be expected in winter, followed by spring. In winter the $PM_{2.5}$ levels could be reduced by 60 μg m^{-3} and even as much as 90 μg m^{-3} in some regions. In contrast, under the increased emission simulations, the $PM_{2.5}$ loadings increased by 13.1–29.3%, and the impacts were particularly obvious in Xi'an. When there was a strong increase in emission sources, the pollution levels increased as much as 100 μg m^{-3}, and the effects were especially strong. Thus winter appears to be the season that would be the most sensitive to pollution emissions and control measures.

These simulations show that the denitrification of industrial coal boilers and the implementation of controls on domestic boilers could have strong effects on $PM_{2.5}$ mass loadings. For the stronger controls scenario, the annual average $PM_{2.5}$ concentration decreased from 85.04 μg m^{-3} to 63.36 μg m^{-3}, but even that reduced level would still be far above the first class of National Ambient Air Quality Standard of 35 μg m^{-3}. In winter, pollutants from upwind sources affect the ambient air but the contribution was not large. This was because the high pollutants levels were mainly the result of strong local emissions which can build up near the earth's surface under the typical wintertime meteorological conditions. Therefore, the control of local emissions will be essential if the air quality standards are to be met for the Guanzhong Plain. In autumn, there is little or no capacity for accommodating additional local emissions because the existing inputs already cause exceedances of the air quality standards.

4. Conclusions

Here we report the seasonal and spatial distributions of $PM_{2.5}$ mass concentrations along with information on the chemical composition of this material at six different locations on the Guanzhong Plain. The study demonstrates the pervasive impacts of anthropogenic emissions on the atmosphere of the region, and it includes an investigation of two pollution episodes, one that occurred in autumn and the other winter. In the urban areas, high SO_4^{2-} levels typically were seen in summer due to the high photochemical activity in that season. The highest NO_3^- concentrations in winter were ascribed to the relatively low temperatures and high emissions of NO_x from both mobile and stationary high-

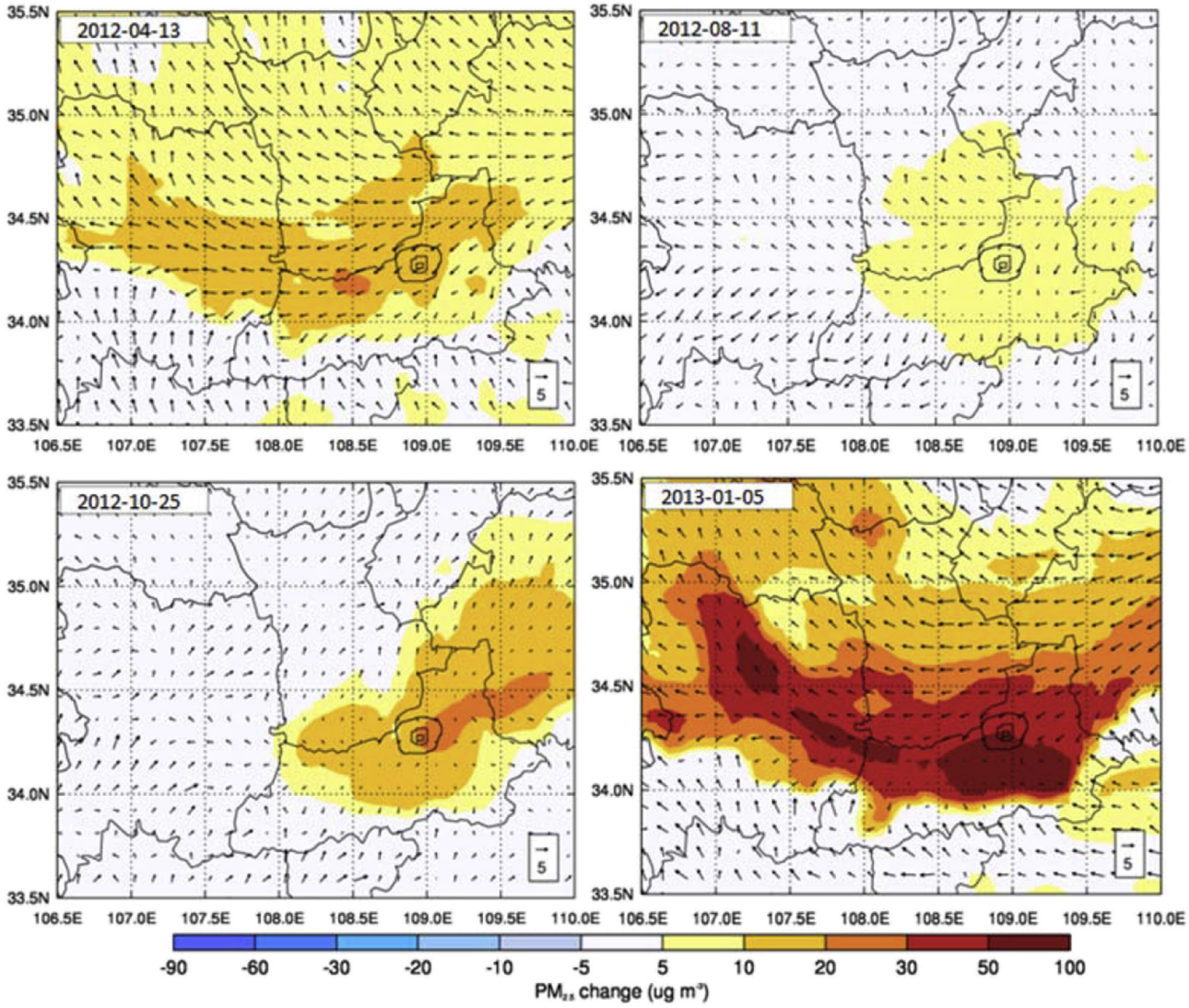

Fig. 6. Effects of strong emission increasing on $PM_{2.5}$ mass concentrations.

temperature combustion sources. The CD values calculated for the chemical constituents indicated a considerable level uniformity of pollution sources over the spatial scale of the study, and there is compelling evidence for strong regional impacts. Secondary aerosol precursors play more critical roles in the formation of SOA than primary sources on Guanzhong plain. The results of simulations with a box model and the WRF-Chem model indicate that strong control measures, that is 20–50% reductions on four major sources (industries, motor vehicles, residences and power-plants), could lead to 13–35% decreases in $PM_{2.5}$ loadings. Differences between the changes in emissions and loadings are due to the transport of pollutants from distance sources, and in fact, pollutants transported into the region had significant effects on air quality, and furthermore, those problems can be compounded by the weak dilution of pollutants by advection and diffusion. Clearly, pollution controls should be tightened to reduce local emissions of both primary PM (particles from the incomplete combustion of coal and biomass, engine exhaust, and fugitive dust) and secondary aerosol precursors (i.e., SO_2, NO_x, and NH_3), but these measures alone with not solve the air pollution problems. That is, it also will be critical to combine these efforts with better management of pollutant emissions from sources upwind.

Acknowledgments

This research was supported by the Shaanxi Government (2012KTZB03-01-01) and projects from “Strategic Priority Research Program” of the Chinese Academy of Science (Grant No. XDB05060500 XDA05100401). The authors wish to thank R. Arimoto for preparing and editing the manuscript.

Appendix A. Supplementary data

Supplementary data related to this article can be found at http://dx.doi.org/10.1016/j.atmosenv.2016.10.029.

References

Andreae, M.O., 1983. Soot carbon and excess fine potassium - long-range transport of combustion-derived aerosols. Science 220, 1148–1151.
Arimoto, R., Duce, R.A., Savoie, D.L., Prospero, J.M., Talbot, R., Cullen, J.D., Tomza, U., Lewis, N.F., Jay, B.J., 1996. Relationships among aerosol constituents from asia and the north pacific during PEM-west a. J. Geophys. Res. Atomos. 101, 2011–2023.
Bi, X.H., Feng, Y.C., Wu, J.H., Wang, Y.Q., Zhu, T., 2007. Source apportionment of PM_{10} in six cities of northern China. Atmos. Environ. 41, 903–912.
Bond, T.C., Streets, D.G., Yarber, K.F., Nelson, S.M., Woo, J.H., Klimont, Z., 2004.

A technology-based global inventory of black and organic carbon emissions from combustion. J. Geophys. Res. Atomos. 109, 43.
Cachier, H., Bremond, M.P., Buat-Menard, P., 1989. Carbonaceous aerosols from different tropical biomass burning sources. Nature 340, 371–373, 19.
Cao, J.J., Zhu, C.S., Ho, K.F., Han, Y.M., Shen, Z.X., Zhan, C.L., Zhang, J.Q., 2015. Light attenuation cross-section of black carbon in an urban atmosphere in northern China. Particuology 18, 89–95.
Cao, J.J., Shen, Z.X., Chow, J.C., Watson, J.G., Lee, S.C., Tie, X.X., Ho, K.F., Wang, G.H., Han, Y.M., 2012a. Winter and summer $PM_{2.5}$ chemical compositions in fourteen chinese cities. J. Air & Waste Manag. Assoc. 62, 1214–1226.
Cao, J.J., Xu, H.M., Xu, Q., Chen, B.H., Kan, H.D., 2012b. Fine particulate matter constituents and cardiopulmonary mortality in a heavily polluted chinese city. Environ. Health Perspect. 120, 373–378.
Cao, J.J., Zhang, T., Chow, J.C., Watson, J.G., Wu, F., Li, H., 2009. Characterization of atmospheric ammonia over Xi'an, China. Aerosol Air Qual. Res. 9, 277–289.
Cao, J.J., Chow, J.C., Watson, J.G., Wu, F., Han, Y.M., Jin, Z.D., Shen, Z.X., An, Z.S., 2008a. Size-differentiated source profiles for fugitive dust in the Chinese Loess Plateau. Atmos. Environ. 42, 2261–2275.
Cao, G., Zhang, X., Gong, S., Zheng, F., 2008b. Investigation on emission factors of particulate matter and gaseous pollutants from crop residue burning. J. Environ. Sci. 20 (1), 50–55.
Cao, J.J., Wu, F., Chow, J.C., Lee, S.C., Li, Y., Chen, S.W., An, Z.S., Fung, K.K., Watson, J.G., Zhu, C.S., Liu, S.X., 2005. Characterization and source apportionment of atmospheric organic and elemental carbon during fall and winter of 2003 in Xi'an, China. Atmos. Chem. Phys. 5, 3127–3137.
Cao, J.J., Lee, S.C., Ho, K.F., Zou, S.C., Fung, K., Li, Y., Watson, J.G., Chow, J.C., 2004. Spatial and seasonal variations of atmospheric organic carbon and elemental carbon in Pearl River Delta Region. China. Atmos. Environ. 38, 4447–4456.
Cao, J.J., Lee, S.C., Ho, K.F., Zhang, X.Y., Zou, S.C., Fung, K., Chow, J.C., Watson, J.G., 2003. Characteristics of carbonaceous aerosol in Pearl River Delta region, China during 2001 winter period. Atmos. Environ. 37, 1451–1460.
Chan, C.K., Yao, X., 2008. Air pollution in mega cities in China. Atmos. Environ. 42, 1–42.
Chen, F., Dudhia, J., 2001. Coupling an advanced land surface-hydrology model with the Penn State-NCAR MM5 modeling system. Part I: model implementation and sensitivity. Mon. Weather Rev. 129, 569–585.
Cheng, Y., Zou, S.C., Lee, S.C., Chow, J.C., Ho, K.F., Watson, J.G., Han, Y.M., Zhang, R.J., Zhang, F., Yau, P.S., Huang, Y., Bai, Y., Wu, W.J., 2011. Characteristics and source apportionment of PM_1 emissions at a roadside station. J. Hazard. Mater. 195, 82–91.
Cheng, Y., Lee, S.C., Ho, K.F., Chow, J.C., Watson, J.G., Louie, P.K.K., Cao, J.J., Hai, X., 2010. Chemically-speciated on-road $PM_{2.5}$ motor vehicle emission factors in Hong Kong. Sci. Total Environ. 408, 1621–1627.
Choi, Y.S., Ho, C.H., Chen, D., Noh, Y.H., Song, C.K., 2008. Spectral analysis of weekly variation in PM_{10} mass concentration and meteorological conditions over China. Atmos. Environ. 42, 655–666.
Chow, J.C., Watson, J.G., Kuhns, H., Etyemezian, V., Lowenthal, D.H., Crow, D., Kohl, S.D., Engelbrecht, J.P., Green, M.C., 2004. Source profiles for industrial, mobile, and area sources in the big bend regional aerosol visibility and observational study. Chemosphere 54, 185–208.
Chow, J.C., Watson, J.G., Pritchett, L.C., Pierson, W.R., Frazier, C.A., Purcell, R.G., 1993. The DRI thermal/optical reflectance carbon analysis system: description, evaluation and applications in U.S. air quality studies. Atmos. Environ. Part a-Gen. Top. 27, 1185–1201.
Duan, F.K., He, K.B., Ma, Y.L., Yang, F.M., Yu, X.C., Cadle, S.H., Chan, T., Mulawa, P.A., 2006. Concentration and chemical characteristics of $PM_{2.5}$ in Beijing, China: 2001-2002. Sci. Total Environ. 355, 264–275.
Duan, F.K., Liu, X.D., Yu, T., Cachier, H., 2004. Identification and estimate of biomass burning contribution to the urban aerosol organic carbon concentrations in Beijing. Atmos. Environ. 38, 1275–1282.
Duan, J.C., Tan, J.H., Hao, J.M., Chai, F.H., 2014. Size distribution, characteristics and sources of heavy metals in haze episod in Beijing. J. Environ. Sci.China 26, 189–196.
Dudhia, J., 1989. Numerical study of convection observed during the winter monsoon experiment using a mesoscale two-dimensional model. J. Atmos. Sci. 46, 3077–3107.
El-Zanan, H.S., Zielinska, B., Mazzoleni, L.R., Hansen, D.A., 2009. Analytical determination of the aerosol organic mass-to-organic carbon ratio. J. Air & Waste Manag. Assoc. 59, 58–69.
El-Zanan, H.S., Lowenthal, D.H., Zielinska, B., Chow, J.C., Kumar, N., 2005. Determination of the organic aerosol mass to organic carbon ratio in IMPROVE samples. Chemosphere 60, 485–496.
Han, B., Zhang, R., Yang, W., Bai, Z.P., Ma, Z.Q., Zhang, W.J., 2016. Heavy haze episodes in Beijing during January 2013: inorganic ion chemistry and source analysis using highly time-resolved measurements from an urban site. Sci. Total Environ. 544, 319–329.
Harrison, R.M., Yin, J.X., 2000. Particulate matter in the atmosphere: which particle properties are important for its effects on health? Sci. Total Environ. 249, 85–101.
Ho, K.F., Cao, J.J., Lee, S.C., Chan, C.K., 2006. Source apportionment of $PM_{2.5}$ in urban area of Hong Kong. J. Hazard. Mater. 138, 73–85.
Ho, K.F., Lee, S.C., Chan, C.K., Yu, J.C., Chow, J.C., Yao, X.H., 2003. Characterization of chemical species in $PM_{2.5}$ and PM_{10} aerosols in Hong Kong. Atmos. Environ. 37, 31–39.
Hu, M., He, L.Y., Zhang, Y.H., Wang, M., Kim, Y.P., Moon, K.C., 2002. Seasonal variation of ionic species in fine particles at Qingdao, China. Atmos. Environ. 36, 5853–5859.
Huang, R.J., Zhang, Y.L., Bozzetti, C., Ho, K.F., Cao, J.J., Han, Y.M., Daellenbach, K.R., Slowik, J.G., Platt, S.M., Canonaco, F., Zotter, P., Wolf, R., Pieber, S.M., Bruns, E.A., Crippa, M., Ciarelli, G., Piazzalunga, A., Schwikowski, M., Abbaszade, G., Schnelle-Kreis, J., Zimmermann, R., An, Z.S., Szidat, S., Baltensperger, U., El Haddad, I., Prevot, A.S.H., 2014. High secondary aerosol contribution to particulate pollution during haze events in China. Nature 514, 218–222.
Kelly, F.J., Fussell, J.C., 2012. Size, source and chemical composition as determinants of toxicity attributable to ambient particulate matter. Atmos. Environ. 60, 504–526.
Kerminen, V.M., Hillamo, R., Teinila, K., Pakkanen, T., Allegrini, I., Sparapani, R., 2001. Ion balances of size-resolved tropospheric aerosol samples: implications for the acidity and atmospheric processing of aerosols. Atmos. Environ. 35, 5255–5265.
Khan, M.F., Shirasuna, Y., Hirano, K., Masunaga, S., 2010. Characterization of $PM_{2.5}$, $PM_{2.5\text{-}10}$ and $PM_{>10}$ in ambient air,Yokohama, Japan. Atmos. Res. 96 (1), 159–172.
Koch, D., 2001. Transport and direct radiative forcing of carbonaceous and sulfate aerosols in the GISS GCM. J. Geophys. Res. Atomos. 106, 20311–20332.
Lai, S.C., Zou, S.C., Cao, J.J., Lee, S.C., Ho, K.F., 2007. Characterizing ionic species in $PM_{2.5}$ and PM_{10} in four Pearl River Delta cities, south China. J. Environ. Sci.China 19, 939–947.
Li, L., Chen, C.H., Fu, J.S., Huang, C., Streets, D.G., Huang, H.Y., Zhang, G.F., Wang, Y.J., Jang, C.J., Wang, H.L., Chen, Y.R., Fu, J.M., 2011. Air quality and emissions in the Yangtze River Delta, China. Atmos. Chem. Phys. 11, 1621–1639.
Lin, Y.L., Farley, R.D., Orville, H.D., 1983. Bulk parameterization of the snow field in a cloud model. J. Clim. Appl. Meteorol. 22, 1065–1092.
Malm, W.C., Schichtel, B.A., Pitchford, M.L., 2011. Uncertainties in $PM_{2.5}$ gravimetric and speciation measurements and what we can learn from Them. J. Air Waste Manag. Assoc. 61, 1131–1149.
Mlawer, E.J., Taubman, S.J., Brown, P.D., Iacono, M.J., Clough, S.A., 1997. Radiative transfer for inhomogeneous atmospheres: RRTM, a validated correlated-k model for the longwave. J. Geophys. Res. Atomos. 102, 16663–16682.
Noh, Y., Cheon, W.G., Hong, S.Y., Raasch, S., 2003. Improvement of the K-profile model for the planetary boundary layer based on large eddy simulation data. Bound. Layer Meteorol. 107, 401–427.
Okuda, T., Okamoto, K., Tanaka, S., Shen, Z., Han, Y., Huo, Z., 2010. Measurement and source identification of polycyclic aromatic hydrocarbons (PAHs) in the aerosol in Xi'an, China, by using automated column chromatography and applying positive matrix factorization (PMF). Sci. Total Environ. 408 (8), 1909–1914.
Shen, G., Yang, Y., Wang, W., Tao, S., Zhu, C., Min, Y., Xue, M., Ding, J., Wang, B., Wang, R., 2010. Emission factors of particulate matter and elemental carbon for crop residues and coals burned in typical household stoves in China. Environ. Sci. Technol. 44 (18), 7157–7162.
Shen, Z.X., Wang, X., Zhang, R.J., Ho, K.F., Cao, J.J., Zhang, M.G., 2011. Chemical composition of water-soluble ions and carbonate estimation in spring aerosol at a semi-arid site of Tongyu, China. Aerosol Air Qual. Res. 11, 360–368.
Shen, Z.X., Cao, J.J., Arimoto, R., Han, Z.W., Zhang, R.J., Han, Y.M., Liu, S.X., Okuda, T., Nakao, S., Tanaka, S., 2009. Ionic composition of TSP and $PM_{2.5}$ during dust storms and air pollution episodes at Xi'an, China. Atmos. Environ. 43, 2911–2918.
Shen, Z.X., Cao, J.J., Arimoto, R., Zhang, R.J., Jie, D.M., Liu, S.X., Zhu, C.S., 2007. Chemical composition and source characterization of spring aerosol over Horqin sand land in northeastern China. J. Geophys. Res. Atomos. 112, 15.
Song, Y., Tang, X.Y., Xie, S.D., Zhang, Y.H., Wei, Y.J., Zhang, M.S., Zeng, L.M., Lu, S.H., 2007. Source apportionment of $PM_{2.5}$ in Beijing in 2004. J. Hazard. Mater. 146, 124–130.
Steinhoff, G., Haupt, O., Dannecker, W., 2000. Fast determination of trace elements on aerosol-loaded filters by X-ray fluorescence analysis considering the inhomogeneous elemental distribution. Fresenius J. Anal. Chem. 366, 174–177.
Strak, M., Janssen, N.A.H., Godri, K.J., Gosens, I., Mudway, I.S., Cassee, F.R., Lebret, E., Kelly, F.J., Harrison, R.M., Brunekreef, B., Steenhof, M., Hoek, G., 2012. Respiratory health effects of airborne particulate matter: the role of particle size, composition, and oxidative potential-the RAPTES project. Environ. Health Perspect. 120, 1183–1189.
Tie, X.X., Cao, J.J., 2010. Aerosol pollution in China: present and future impact on environment. Particuology 7, 426, 2009). 8, 79–79.
van Donkelaar, A., Martin, R.V., Brauer, M., Kahn, R., Levy, R., Verduzco, C., Villeneuve, P.J., 2010. Global estimates of ambient fine particulate matter concentrations from satellite-based aerosol optical depth: development and application. Environ. Health Perspect. 118, 847–855.
Vega, E., Reyes, E., Ruiz, H., Garcia, J., Sanchez, G., Martinez-Villa, G., Gonzalez, U., 2004. Analysis of $PM_{2.5}$ and PM_{10} in the atmosphere of Mexico city during 2000-2002. J. Air Waste Manag. Assoc. 54, 786–798.
Watson, J.G., Chow, J.C., Houck, J.E., 2001. $PM_{2.5}$ chemical source profiles for vehicle exhaust, vegetative burning, geological material, and coal burning in northwestern Colorado during 1995. Chemosphere 43, 1141–1151.
Wang, D.X., Hu, J.L., Xu, Y., Lv, D., Xie, X.Y., Kleeman, M., Xing, J., Zhang, H.L., Ying, Q., 2014. Source contributions to primary and secondary inorganic particulate matter during a severe wintertime $PM_{2.5}$ pollution episode in Xi'an, China. Atmos. Environ. 97, 182–194.
Wang, P., Cao, J.J., Shen, Z.X., Han, Y.M., Lee, S.C., Huang, Y., Zhu, C.S., Wang, Q.Y., Xu, H.M., Huang, R.J., 2015. Spatial and seasonal variations of PM2.5 mass and species during 2010 in Xi'an, China. Sci. Total Environ. 508, 477–487.
Wang, T.J., Jiang, F., Deng, J.J., Shen, Y., Fu, Q.Y., Wang, Q., Fu, Y., Xu, J.H., Zhang, D.N.,

2012. Urban air quality and regional haze weather forecast for Yangtze River Delta region. Atmos. Environ. 58, 70–83.
Wang, Y., Zhang, Q.Q., He, K., Zhang, Q., Chai, L., 2013. Sulfate-nitrate-ammonium aerosols over China: response to 2000-2015 emission changes of sulfur dioxide, nitrogen oxides, and ammonia. Atmos. Chem. Phys. 13, 2635–2652.
Wang, Y., Zhuang, G.S., Tang, A.H., Yuan, H., Sun, Y.L., Chen, S.A., Zheng, A.H., 2005. The ion chemistry and the source of $PM_{2.5}$ aerosol in Beijing. Atmos. Environ. 39, 3771–3784.
Wang, Y.Q., Zhang, X.Y., Arimoto, R., 2006. The contribution from distant dust sources to the atmospheric particulate matter loadings at XiAn, China during spring. Sci. Total Environ. 368, 875–883.
Wesely, M.L., 1989. Parameterization of surface resistance to gaseous dry deposition in regional-scale numerical models. Atmos. Environ. 23, 1293–1304.
Wongphatarakul, V., Friedlander, S.K., Pinto, J.P., 1998. A comparative study of $PM_{2.5}$ ambient aerosol chemical databases. Environ. Sci. Technol. 32, 3926–3934.
Wu, F., Chow, J.C., An, Z.S., Watson, J.G., Cao, J.J., 2011. Size-Differentiated chemical characteristics of asian paleo dust: records from aeolian deposition on chinese loess plateau. J. Air Waste Manag. Assoc. 61, 180–189.
Xiao, S., Wang, Q.Y., Cao, J.J., Huang, R.J., Chen, W.D., Han, Y.M., Xu, H.M., Liu, S.X., Zhou, Y.Q., Wang, P., Zhang, J.Q., Zhan, C.L., 2014. Long-term trends in visibility and impacts of aerosol composition on visibility impairment in Baoji, China. Atmos. Res. 149, 88–95.
Xu, H.M., Cao, J.J., Ho, K.F., Ding, H., Han, Y.M., Wang, G.H., Chow, J.C., Watson, J.G., Khol, S.D., Qiang, J., Li, W.T., 2012. Lead concentrations in fine particulate matter after the phasing out of leaded gasoline in Xi'an, China. Atmos. Environ. 46, 217–224.
Yang, F., Tan, J., Zhao, Q., Du, Z., He, K., Ma, Y., Duan, F., Chen, G., Zhao, Q., 2011. Characteristics of PM2.5 speciation in representative megacities and across China. Atmos. Chem. Phys. 11, 5207–5219.
Zeng, T., Wang, Y.H., 2011. Nationwide summer peaks of OC/EC ratios in the contiguous United States. Atmos. Environ. 45, 578–586.
Zhai, Y.B., Liu, X.T., Chen, H.M., Xu, B.B., Zhu, L., Li, C.T., Zeng, G.M., 2014. Source identification and potential ecological risk assessment of heavy metals in $PM_{2.5}$ from Changsha. Sci. Total Environ. 493, 109–115.
Zhang, N.N., Cao, J.J., Ho, K.F., He, Y.Q., 2012. Chemical characterization of aerosol collected at Mt. Yulong in wintertime on the southeastern Tibetan Plateau. Atmos. Res. 107, 76–85.
Zhang, T., Cao, J.J., Tie, X.X., Shen, Z.X., Liu, S.X., Ding, H., Han, Y.M., Wang, G.H., Ho, K.F., Qiang, J., Li, W.T., 2011. Water-soluble ions in atmospheric aerosols measured in Xi'an, China: seasonal variations and sources. Atmos. Res. 102, 110–119.
Zhang, X.X., Shi, P.J., Liu, L.Y., Tang, Y., Cao, H.W., Zhang, X.N., Hu, X., Guo, L.L., Lue, Y.L., Qu, Z.Q., Jia, Z.J., Yang, Y.Y., 2010. Ambient TSP concentration and dustfall in major cities of China: spatial distribution and temporal variability. Atmos. Environ. 44, 1641–1648.
Zhao, X.J., Zhao, P.S., Xu, J., Meng, W., Pu, W.W., Dong, F., He, D., Shi, Q.F., 2013. Analysis of a winter regional haze event and its formation mechanism in the North China Plain. Atmos. Chem. Phys. 13, 5685–5696.
Zhang, X.Y., Wang, Y.Q., Zhang, X.C., Guo, W., Gong, S.L., 2008. Carbonaceous aerosol composition over various regions of China during 2006. J. Geophys. Res. Atomos. 113, 10.
Zhang, X.Y., Cao, J.J., Li, L.M., Arimoto, R., Cheng, Y., Huebert, B., Wang, D., 2002. Characterization of atmospheric aerosol over XiAn in the south margin of the loess plateau, China. Atmos. Environ. 36, 4189–4199.
Zhu, C.S., Cao, J.J., Tsai, C.J., Shen, Z.X., Han, Y.M., Liu, S.X., Zhao, Z.Z., 2014. Comparison and implications of $PM_{2.5}$ carbon fractions in different environments. Sci. Total Environ. 466, 203–209.
Zhu, C.S., Cao, J.J., Tsai, C.J., Shen, Z.X., Ho, K.F., Liu, S.X., 2010. The indoor and outdoor carbonaceous pollution during winter and summer in rural areas of Shaanxi, China. Aerosol Air Qual. Res. 10, 550–558.